AIP | APL Materials

Morphology-controlled growth of perylene derivative induced by double-hydrophilic block copolymers

Minghua Huang, Markus Antonietti, and Helmut Cölfen

Citation: APL Mater. **4**, 015705 (2016); doi: 10.1063/1.4934704
View online: http://dx.doi.org/10.1063/1.4934704
View Table of Contents: http://scitation.aip.org/content/aip/journal/aplmater/4/1?ver=pdfcov
Published by the AIP Publishing

Morphology-controlled growth of perylene derivative induced by double-hydrophilic block copolymers

Minghua Huang,[1,2] Markus Antonietti,[2] and Helmut Cölfen[2,3,a]
[1]*Institute of Materials Science and Engineering, Ocean University of China, Qingdao 266100, China*
[2]*Colloid Chemistry, Max-Planck-Institute of Colloids and Interfaces, Research Campus Golm, D-14424 Potsdam, Germany*
[3]*Physical Chemistry, University of Konstanz, Universitätsstr. 10, D-78457 Konstanz, Germany*

(Received 11 July 2015; accepted 14 October 2015; published online 9 November 2015)

Controlled growth of technically relevant perylene derivative 3, 4, 9, 10-perylene-tetracarboxylic acid potassium salt (PTCAPS), with tuneable morpologies, has been successfully realized by a recrystallization method using a double-hydrophilic block copolymer poly (ethylene glycol)-block poly (ethyleneimine) (PEG-b-PEI) as the structure directing agent. The {001} faces of PTCAPS are most polar and adsorb the oppositively charged polymer additive PEG-b-PEI well by electrostatic attraction. By simply adjusting the PEG-b-PEI concentration, systematic morphogenesis of PTCAPS from plates to microparticles composed of various plates splaying outwards could be realized. Furthermore, the variation of pH value of the recrystallization solution could induce the change of the interaction strength between PEG-b-PEI additive and PTCAPS and thus modify the morphology of PTCAPS from microparticles composed of various plates to ultralong microbelts. [http://dx.doi.org/10.1063/1.4934704]

Fabrication of functional nano- and microsized materials with well-defined shapes, size, and dimensionalities receive increasing attention worldwide, because of their promising applications in various fields such as catalysis, medicine, electronics, ceramics, and pigments.[1] In the past few years, inorganic functional materials with controlled superstructures have been extensively fabricated, such as titania, zinc oxide, calcium carbonate, and so on.[2] Compared to inorganic systems, the morphosynthesis of organic systems is less developed, but due to the high flexibility both in their physicochemical and self-assembly properties may access a wider range of electrical and optical properties. From this viewpoint, it is of both scientific and technological interests to fabricate crystalline organic functional materials with the desired size and shapes, ideally in an extent as it was already accomplished for the inorganic counterparts. The controlled manipulation of different morphologies of organic functional materials however remains a great challenge.

Uniformly shaped organic nanorods and nanospheres have been fabricated by the self-aggregation of different stilbazolium dyes,[3] but also nanospheres, square nanowires, and nanocubes were prepared from three isomeric molecules, respectively.[4] Another remarkable exception is the recent fabrication of one-dimensional structures from large planar aromatic molecules.[5] Different supramolecular structures of ionic perylene bisimides have been manipulated by ionic self-assembly (ISA).[6] Also using different derivatives of perylene diimide, nanobelts, and nanospheres were fabricated by a solvent displacement process.[7] In these cases, the formations of organic superstructures with distinct shapes are realized by the modification of the organic molecules as such. For example, the molecular structure of perylene diimide is modified by adding different long alkyl chains, in order to obtain a balance to the strong stacking interactions of the dye cores with the hydrophobic interactions of the side chains, which in turn leads to the formation of organic superstructures with distinct shapes.

[a]Author to whom correspondence should be addressed. Electronic mail: helmut.coelfen@uni-konstanz.de

When the molecule to crystallize is fixed, additive-controlled crystallization is one of the most important techniques that have been proven successful in forming various hierarchical superstructures of inorganics.[8] As nucleation and growth are very sensitive processes, crystallization is usually modified by various additives such as surfactants, biopolymers, and synthetic macromolecules, etc.[9] Our group has specialized on polymer-induced crystallization to develop the morphosynthesis of inorganic salts, especially biominerals, including the control of size, shape, polymorph, and hierarchical superstructure.[9(c)-9(f)] The influence of polymers on crystal formation is usually attributed to their selective adsorption and/or enrichment onto specific crystal faces, similar to that seen with low molecular weight ionic compounds, which in turn then inhibit the growth of these faces.[10] However, recent investigations show that additives can already influence crystallization before a nucleation event takes place by influencing stable pre-nucleation clusters,[11] which was evidenced for $CaCO_3$.

Particularly effective steric stabilizers for inorganic crystals in aqueous systems are the so-called double-hydrophilic block copolymers (DHBCs), which consist of a hydrophilic block designed to interact strongly with appropriate inorganic minerals and surfaces, and another hydrophilic block that mainly promotes solubilisation in water.[12] Compared to inorganic superstructures, controlled crystallization of organic crystals with defined shapes by the addition of surfactants, dendrimers, and synthetic polymers has so far had only limited success.[13] Very polar organic crystals such as amino acids[14] and also organic pigments[15] have indicated a certain potential, but to our opinion it is still a challenge to use this principle to fabricate other kinds of novel organic crystals.

In the present work, a perylene derivative, a π-conjugated aromatic dye molecule, was selected as a model system. Perylene derivatives have high relevance as one of the most extensively studied classes of organic n-type semiconductors with good fluorescent properties and high photostability, in contrast to the more common p-type organic semiconductors. They have been widely utilized as unique candidates for the fabrication of organic optoelectronic devices.[16] Thus, the fabrication of such functional organic micro- and nanostructures with controlled sizes and shapes is of potential application interest. Herein, we report the different morphological evolution with well-defined shapes from the same organic molecule by using the principles of polymer controlled crystallization.

All chemicals were of analytical grade and used as received without further purification. Perylene 3, 4, 9, 10-tetracarboxylic dianhydride was purchased from Aldrich. 3, 4, 9, 10-perylenetetracarboxylic acid potassium salt (PTCAPS) was synthesized as previously reported.[17] Poly (ethylene glycol)-block poly(ethyleneimine) (PEG-b-PEI-branch, weight average molecular weight, M_w of PEG = 5000 g mol^{-1}; M_w of ethyleneimine = 1200 g mol^{-1}) was also synthesized as previously reported via the epoxide route after prior removal of low molar mass PEI impurities by dialysis with Molecular Weight Cutoff (MWCO) 1000 g mol^{-1}.[18]

All glassware was cleaned and sonicated in ethanol for 5 min, after rinsed with distilled water and further soaked with a H_2O-HNO_3(65%)-H_2O_2(1:1:1 v/v/v) solution, then rinsed with distilled water, and finally dried in air with acetone.

Control of the morphologies of PTCAPS assemblies in a mixed solvent was achieved by using the following facile recrystallization method. In a typical procedure, 40 mg of PTCAPS and 4 mg PEG-b-PEI (1.0 g/L) were added to 4 ml mixed solvents (0.0015M HCl: ethanol 5:7) in a glass bottle. The PTCAPS solution was then heated to 65 °C for 10 min under magnetic stirring. A small glass substrate was put on the bottom of the glass bottle. Finally, the bottle was allowed to cool naturally to ambient temperature without stirring. After crystallization, the glass substrate was removed from the solution and washed for several times with acetone very quickly. Crystals were collected after 2 and 24 h, which resulted in different morphologies in the additive free reference experiment but identical morphologies in the presence of additives. The crystals on the glass substrates are used for SEM measurements. To investigate the role of experimental parameters on the crystal morphologies, the concentration of the copolymer and the starting pH was varied. The pH of the solution was changed to a defined value from 9.6, 8.4, and 8.1 by changing the concentration of HCl such as 0.0015, 0.008, and 0.01M, respectively. pH 10.3 was realized by using 0.0015M KOH instead of HCl. For the microbelt formation at pH 8.4 or 8.1, after crystallization for several days, the crystals were isolated by filtering and carefully washed three times with ethanol, then dried at 40 °C under vacuum.

For the morphology characterization of the PTCAPS crystals, the SEM measurements were performed on a LEO 1550-Gemini. The SEM samples were coated with a layer of palladium directly to

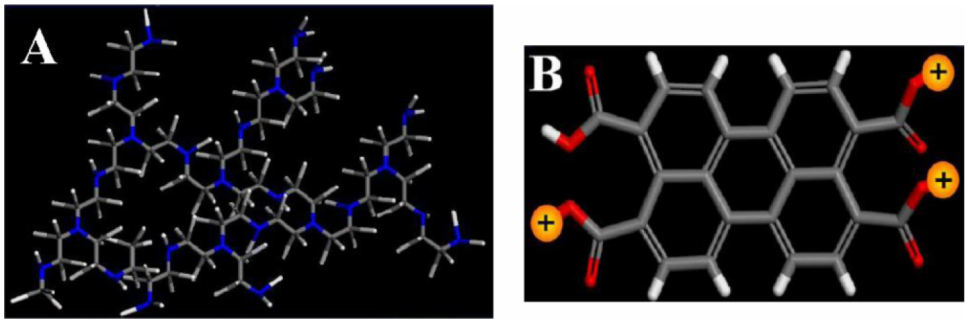

SCHEME 1. The chemical structures of (a) branched PEI (the PEG block was omitted for the sake of clarity) and (b) PTCAPS. The cations are K^+.

improve the sample conductivity. The light microscopy image was taken in solution with an Olympus BX50 microscope. Powder X-ray diffraction (XRD) was measured in the reflection mode (Cu K_α radiation) on a Bruker D8 diffractometer equipped with a scintillation counter. The SEM measurements were performed on a LEO 1550 Gemini microscope.

The ORTEP plot and the molecular structure of the perylenetetracarboxylate anion were generated with the program DIAMOND Vers. 31. (Crystal Impact). The unit cell structure was visualized using Mercury Vers. 2.2. and the modeling of the morphology (Module Morphology) as well as surface cleavage (Visualizer) were performed with the Materials Studio 4.3. software (Accelrys). Wide-angle X-ray scattering (WAXS) patterns were also simulated with the Materials Studio 4.3. software (Accelrys) using the Reflex module.

A cationic double-hydrophilic block copolymer, PEG-b-PEI (weight average molecular weight, M_w of PEG = 5000 g mol^{-1}; M_w of ethyleneimine = 1200 g mol^{-1}) that consists of a binding PEI block and a solvating PEG block (Scheme 1(a)) was used as crystal growth modifier where the growth of oppositely charged 3, 4, 9, 10-PTCAPS is affected to give a variety of well-defined morphologies. The chemical structure of PTCAPS and PEI is shown in Scheme 1. Based on pH titration results, one carboxylic acid group was still protonated and only 3 groups in the salt form.[19] Because the solubility of PTCAPS in water is very high and it is practically insoluble in many organic media, we used a facile recrystallization method to prepare crystals of PTCAPS from ethanol/water mixed solvents. The precursor PTCAPS molecules dissolve in mixed solvents at higher temperature and precipitate as the temperature decreases because the solution is supersaturated at the lower temperature.

In this experiment, 40 mg PTCAPS were dispersed in 4 ml ethanol/water mixed solvents and dissolved to get 10 g/L solution at elevated temperature of 65 °C. The solution was allowed to cool naturally to ambient temperature without stirring. In the absence of the polymer additive PEG-b-PEI (the default experiment), the precipitation rate was very fast. The mixed solution always became turbid in less than 15 min. Figure 1 shows the SEM images of the morphologies of PTCAPS crystals obtained by the recrystallization method without any additive at different time scales. Irregular elongated needle-like crystals with a size of 30–600 μm were obtained within 2 h (Figure 1(a)). At

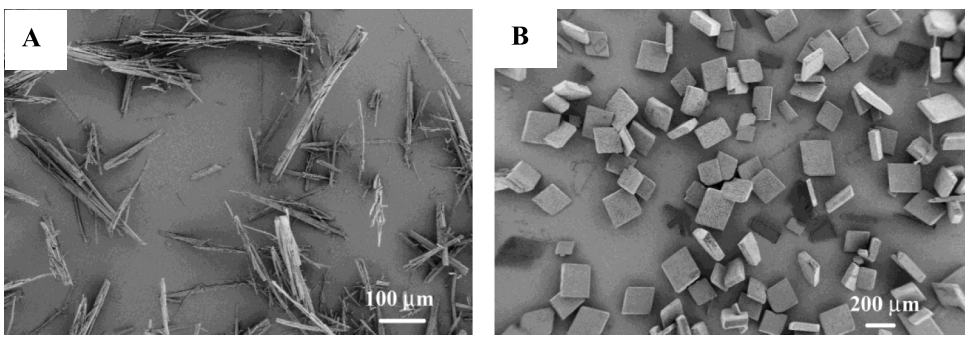

FIG. 1. Typical SEM images of PTCAPS crystallized within 2 h (a), and 24 h (b) in the absence of polymer additive.

longer time scales, after aging in the mother solution for about 24 h at room temperature, these needle-like crystals transfer into rhombohedral tile-shaped crystals with a size of 100-300 μm as shown in Figure 1(b). These results imply that the initially needle shaped crystals are a metastable α-polymorph. This transforms into the stable β-polymorph, which may be attributed to kinetic and thermodynamic polymorphs. In fact, it was reported that perylene has both the α and β polymorphs.[16(b)] The single crystal structure of the stable PTCAPS β-polymorph has been published previously,[19] while we were not able to collect a big-enough single crystal of the α-polymorph being stable long enough to determine its single crystal structure.

The WAXS diffractograms of the two polymorphs are given in Figure 2. It can be seen that the diffractogram for the β-polymorph platelets shows different peak intensities due to orientational effects. The (001) peak is less intense than in the reference. On the other hand, the (10-1) and (20-2) peaks for the side faces are more pronounced. Also (20-3) and (30-3) are more pronounced than in the calculated reference data. This indicates orientational effects, since most of the platelets with exposed {001} faces lie flat on the sample holder (see also Figure 1(b)).

The rhombohedral plate morphology of the β-polymorph corresponds to the equilibrium morphology, which was calculated on basis of the single crystal structure of the β-polymorph.[19] The unit cell parameters are a = 7.4228(14) Å, b = 8.1929(18) Å, c = 14.838(4) Å, α = 104.299(18)°, β = 100.577(18)°, γ = 95.938(7)°. The expected equilibrium morphology as well as the growth directions is presented in Figure 3. It can be seen that the {001} faces get predominantly exposed in the morphology. Figure 3(c) shows that the PTCAPS molecule has a tilted position towards all of the expressed faces. However, {001} is the most polar face with expressed carboxyl groups, which can be addressed by a cationic additive like PEG-b-PEI. The growth directions of the crystal are mainly along its edges (Figure 3(c)). Thus, none of these faces gets larger upon growth.

Completely different morphologies are obtained when the double-hydrophilic block copolymer PEG-b-PEI is used as crystal growth modifier for the crystallization of PTCAPS molecules. In the presence of PEG-b-PEI, the crystal obtained at 2 and 24 h are morphologically same, which is different with that of the control crystal. The sample was prepared by cooling down the mixture ethanol/water solution containing 10 g/l PTCAPS and 1.0 g/L PEG-b-PEI from 65 °C to room temperature without stirring. The pH value of the PTCAPS solution at 65 °C is about 9.6. The addition of 1.0 g/L PEG-b-PEI to the PTCAPS crystallization mixture prolonged the primary crystallization process, and large amounts of precipitate were formed within several hours. Figure 4 shows the SEM images of these modified PTCAPS crystals. Almost identical, chrysanthemum-like assemblies with a diameter of about 150 μm were obtained. A high-magnification image of a single flower revealed that the assemblies were constructed from nanoplates with a thickness of about 500-1000 nm. At pH 9.6, PEG-b-PEI is slightly positively charged (pKa of PEI 10-11)[20] and PTCAPS negatively charged.[19] Therefore, PEG-b-PEI can interact with PTCAPS by electrostatic interaction and adsorb onto the negatively charged {001} faces. This leads to blocking of these faces from further growth,

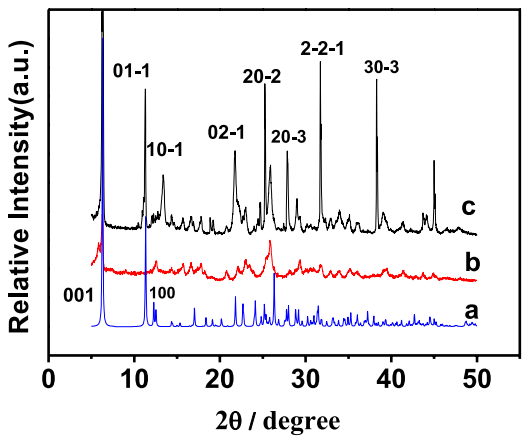

FIG. 2. WAXS patterns of PTCAPS. Calculated curve on basis of the single crystal structure of the tile-like β-polymorph[19] (a), needle-like PTCAPS crystal (α-polymorph) experimental (b), and tile-like crystals (β-polymorph) experimental (c).

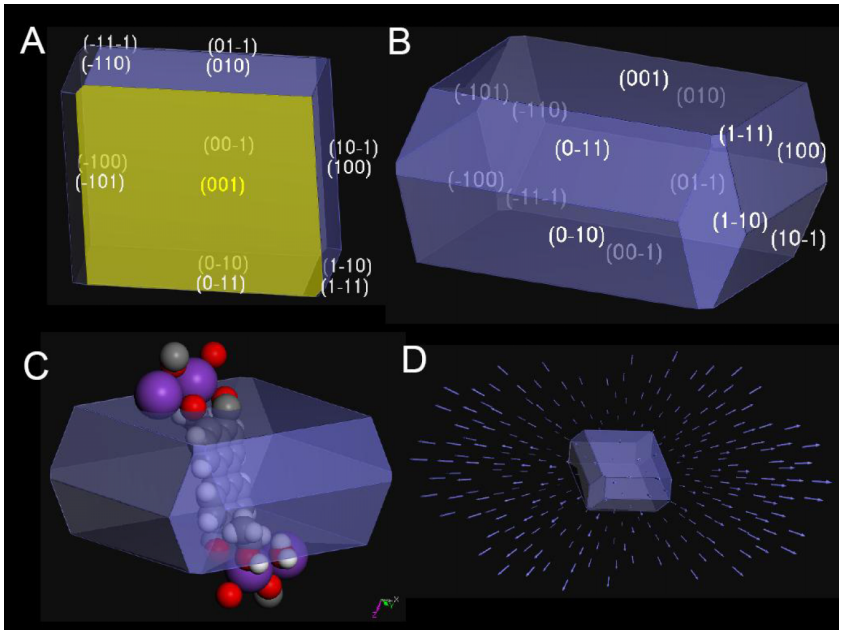

FIG. 3. Equilibrium morphologies calculated for PTCAPS ((a) and (b)) using Materials Studio MS-Modelling (Accelrys). The faces are indexed. In (a), (001) is marked in yellow to show the rhombohedral shape (c) shows the equilibrium morphology including the PTCAPS molecule (not drawn to scale). Grey = carbon, white = hydrogen, red = oxygen, and purple = potassium. The growth faces are shown in (d) where the size of the arrows represents the growth speed into the respective direction.

as the surface energy gets lowered, and further exposition of {001} in the default morphology according to Wulffs rule[21] to yield very thin plates, which are the primary building units of the structures in Figure 4.

The growth of the microparticles composed of roughly radially arranged platelets can be understood from a primary nucleation event of a PTCAPS crystal platelet with β-polymorph. Polymer adsorption will essentially lead to 2D growth while secondary heterogeneous nucleation on the plate surface will lead to the generation of further platelets, with an angle to the primary platelet, which will segment the space for further heterogeneously nucleated platelets (see circles in Figure 4(b)). This will finally lead to the almost radial splay out of the platelets, each of which essentially grows in two dimensions (Figure 4(b)). Particles, which can be seen from the side in Figure 4(a) show an almost constant width of the plates. This can be attributed to the different surface structures of {100} and {010} (see Figure 5). As {100} exposes easier accessible negatively charged carboxy groups (Figure 5) as compared to {010}, PEO-b-PEI will preferably adsorb on {100} thus inhibiting the

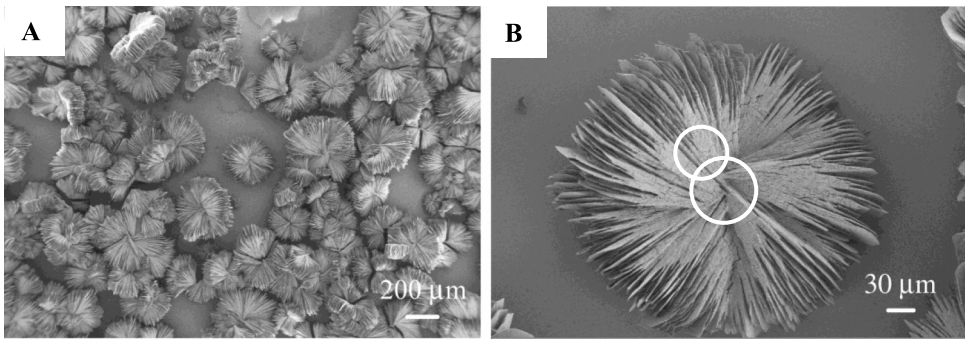

FIG. 4. Typical SEM images of PTCAPS crystal at low magnification (a) and high magnification (b) in the presence of 1.0 g/l PEG-b-PEI. pH = 9.6. The circles show examples where secondary heterogenous nucleation took place.

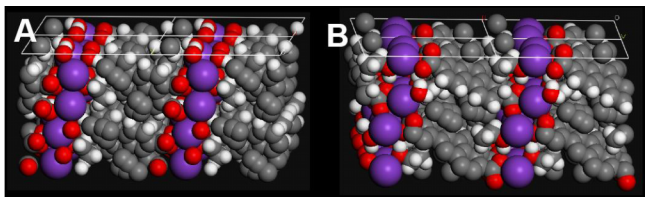

FIG. 5. Surface cleavage of PTCAPS of (a) (100) and (b) (010). The white rectangle is the cleavage surface of each unit cell. Grey = carbon, white = hydrogen, red = oxygen, and purple = potassium. {100} has easier accessible carboxyl groups.

growth of this face more than {010} leading to the observed highly directional growth of the two side faces of the platelet.

To clarify the role of the polymer additive PEG-b-PEI on the morphology control of organic crystals, the polymer concentration was varied while keeping the other experimental conditions unchanged. It is found that the obtained crystal morphologies strongly depend on the concentration of PEG-b-PEI. In the presence of a very low polymer concentration (0.1 g/L), irregular nanoplatelet aggregates were obtained, and their size distribution was rather broad, as shown in Figures 6(a)

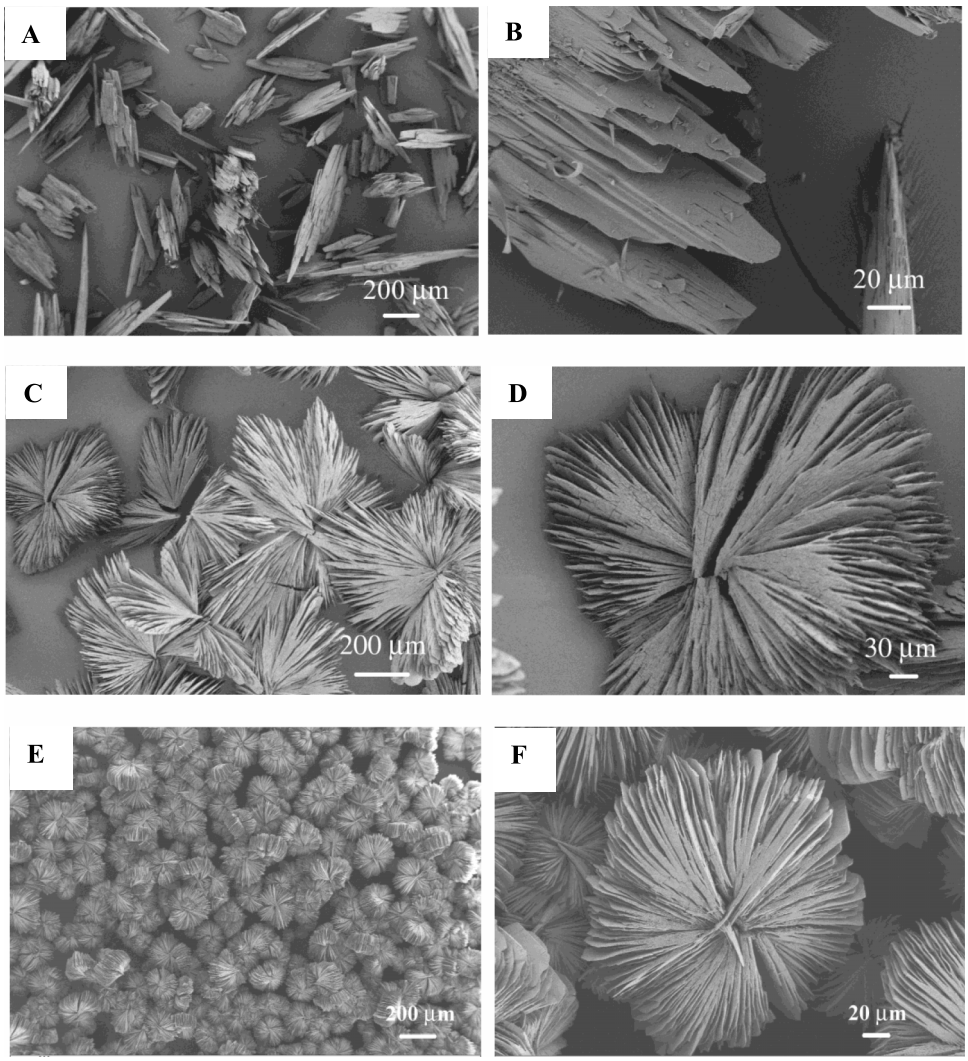

FIG. 6. Typical SEM images of PTCAPS crystals prepared in the presence of PEG-b-PEI with different concentrations. ((a) and (b)) 0.1 g/L, pH = 9.0; ((c) and (d)) 0.4 g/l, pH = 9.3; ((e) and (f)) 2.0 g/l. pH = 9.9.

and 6(b). The thickness of an individual nanoplatelet is here about 1–5 μm, in good agreement with the proposed role of the modifier. When the polymer concentration was 0.4 g/L, the crystals turned into a stack-of-plate superstructure with a size of about 320 μm and platelet thickness of ca. 1 μm (Figures 6(c) and 6(d)), which is bigger than that of the flowerlike structures prepared at higher polymer PEG-b-PEI concentrations such as 1.0 g/L (Figures 6(e) and 6(f)). The dimensions of the individual platelets are different and the microparticles are segmented, which shows that the individual parts of the microparticles nucleated at different times. If the polymer concentration was further increased to 2.0 g/L, there was only minor change for the morphology of the obtained crystals. As shown in Figures 6(e) and 6(f), flower-like uniform structures with 200 μm size were obtained, high-magnification SEM images indicated that the flowers were constructed by nanoplates with a thickness of around 500 nm. Therefore, depending on experimental conditions, the growth of crystal morphologies involves a multistage process with plates as identifiable subunits. The higher the polymer additive PEG-b-PEI concentration, the thinner are the plates, and the more pronounced is secondary heterogeneous nucleation, which is evident in the number of branching plates. This observation goes well with the different polymer PEG-b-PEI concentration on {001}, which blocks the growth of this face to a different extent and thus controls the plate thickness. On the other hand, the positively charged polymer PEG-b-PEI can also serve as a nucleation spot by enhancing the local PTCAPS concentration and therefore leading to heterogeneous nucleation of secondary plates.

Variation of pH of the recrystallization solution can drastically change the morphologies of the produced PTCAPS crystals as this tunes the electrostatic polymer-crystal interaction (the concentration of the polymer additive PEG-b-PEI is fixed constant at 1.0 g/L). Decreasing pH to pH 8.4, which led to an increased polymer—PTCAPS interaction, resulted in interesting fibrous structures (Figure 7).[19] Optical microscopy and SEM measurement showed that microbelt structures with lengths of up to the centimetre range were formed (Figures 7(a) and 7(b)).

If the pH was further decreased to 8.1, there is almost no change for the morphology of the ultralong microbelts structures. Such one-dimensional nanostructures are very interesting for the construction of integrated nanoelectronic devices, as they might, for instance, provide the n-conduction pathways in organic solar cells and photodiodes. While the crystal structures, which are obtained at pH 9.6 are single crystals for which a flat cleavage plane is expected (see Figure S1[22]), the ultralong microbelts are fracturing in a very particulate manner, i.e., they were found to be mesocrystals, which are composed of nanoparticles.[19] These structures will not be further discussed here but the fact that a crystallization mechanism can change from classical crystallization (here at pH 9.6) to nonclassical particle based crystallization (here at pH 8.1–8.4) is similar to the pH dependent crystallization of alanine.[14(d)] Here, at a lower pH such as pH 8.4, as shown in Figure S2,[22] the crystallization of PTCAPS is more inhibited by the additive PEO-b-PEI so that a higher supersaturation is reached until nucleation of a large number of nanoparticles occurs. Such situation will lead to mesocrystal formation while slower crystallization at lower supersaturation leads to single crystal formation with surface energy controlled morphology tuned by polymer adsorption.

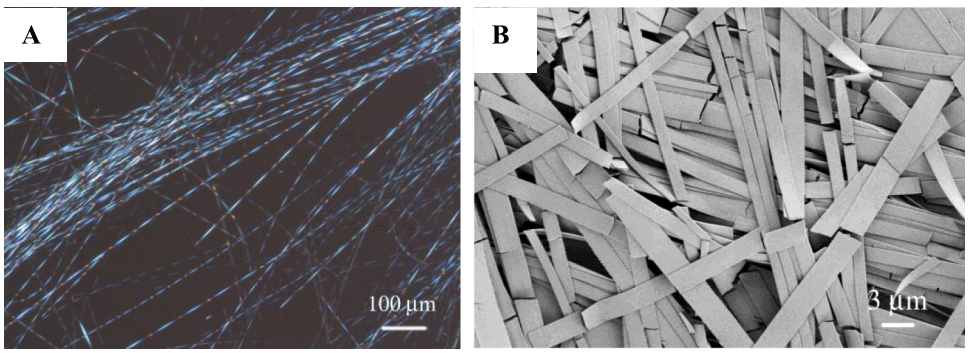

FIG. 7. (a) Polarized light microscopy images (scale bar: 100 μm), and (b) SEM images of PTCAPS crystal in the presence of 1.0 g L^{-1} PEG-b-PEI, pH = 8.4, scale bar: 3 μm.

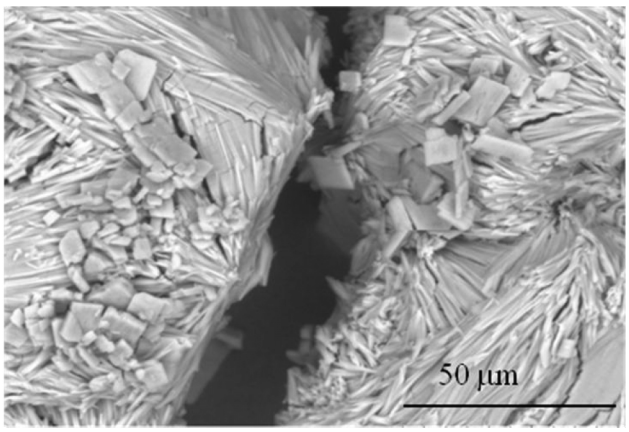

FIG. 8. PTCAPS crystals obtained at pH 10.3. The polymer PEG-b-PEI concentration is fixed at 1.0 g/L PEG-b-PEI.

The above results show the strong directing influence of PEO-b-PEI on the crystallization of PTCAPS, which in addition is pH tuneable. A further proof can be provided if the pH value of the crystallization experiment is increased to 10.3 by KOH (polymer PEG-b-PEI concentration is fixed at 1.0 g/L PEG-b-PEI). Rectangular, noodle-like plate crystal shapes were obtained (Figure 8), which are similar to those of the PTCAPS crystals obtained without polymer additive (Figure 1(b)). In this case, PEG-b-PEI and PTCAPS molecules were both in the deprotonated form and no electrostatic attraction between PEG-b-PEI and PTCAPS molecules is operative, anymore.

In addition to the thermal recrystallization approach described above, another direct precipitation method to crystallize perylene derivatives was used. Due to the fact that the solubility of 3, 4, 9, 10-perylenetetracarboxylic acid sodium salt (PTCASS) is lower than that of PTCAPS, the PTCAPS will precipitate after the addition of sodium ions into the solution of PTCAPS. As shown in Figure 9(a), needle-like crystals were observed in the absence of the polymer additive. We also found

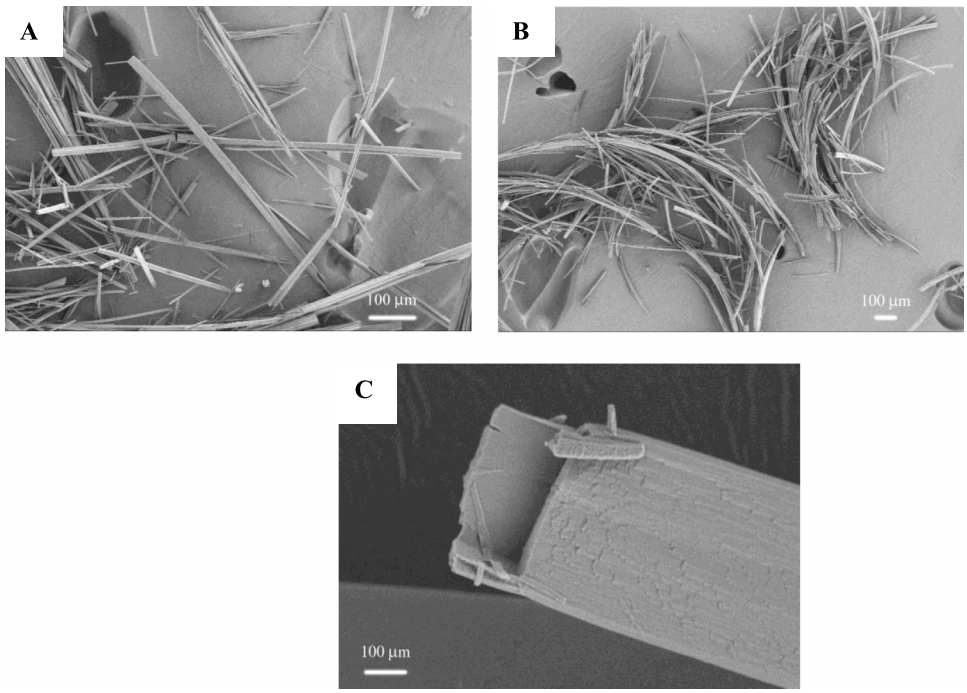

FIG. 9. (a) SEM image of PTCASS precipitated after addition of sodium ions to a PTCAPS solution in absence of polymer, ((b) and (c)) SEM images of hollow tubes of PTCAPS in the presence of PEG-b-PEI.

that no crystallization occurred with the addition of potassium ions into the solution of PTCAPS, which excluded salting out by the increase of the ionic strength. PTCAPS and PTCASS crystals are very difficult to isolate as they quickly dissolve upon ethanol evaporation in the solvent becoming richer in water. Therefore, a rapid drying and isolation procedure was established. The crystallization rate of PTCAPS was decreased with the addition of PEG-b-PEI. As shown in Figures 9(b) and 9(c), curved hollow microtubes were obtained, which are morphologically similar to DL-alanine hollow tubes that were formed in the presence of structure directing additive DHBCs.[13(d)] This shows that the formation of hollow tubes from unstable precursor species is a more general phenomenon for organic molecules.

In conclusion, the manipulation of different morphologies of PTCAPS has been successfully realized by using polymer controlled crystallization principles. Various structures of PTCAPS have been fabricated by using the copolymer PEG-b-PEI as the structure directing agent, which can adsorb predominantly onto the {001} faces of PTCAPS. Such adsorption is very similar to the already well-known formation of complexes by ISA.[6] However, the complex formation by binding of the polymer additive is highly localized and face selective and therefore allows for morphology tuning.

Knowledge of the single crystal structure allows identifying possible additive adsorption sites. The systematic morphogenesis from plates to microparticles composed of various plates splaying outwards could be realized by simple change of the polymer concentration and thus the concentration of the selectively adsorbing additive. The important feature of the here presented system is that the interaction strength between the polymer additive and PTCAPS crystal could be tuned by a simple variation of the pH from nonbinding (pH 10.3) via weakly binding at pH 9.6 to strongly binding at pH 8.1–8.4. Stronger binding of the polymer additive at pH 8.1–8.4 led to the formation of ultralong microbelts. Further acidification is not possible, as it leads to protonation of the perylene species and coupled complete insolubility.

This study shows that face selective polymer adsorption, which is well established for the morphogenesis of inorganic crystals[8] can also be successfully applied to the morphogenesis of functional organic molecules. In fact, molecules like PTCAPS are even much better suited for face selective adsorption of a functional additive, as the crystal is composed of molecules, which will have different expositions of their functionalities at different crystal faces. In the case of PTCAPS, the {001} faces are the most polar ones, which are well suited for the adsorption of a counter charged additive by electrostatic attraction.

This adsorption determines also the morphogenesis of the next structural level of platelet assemblies. Therefore, morphologies and thus properties of a functional organic molecule can be fine-tuned by experimental variables as simple as pH and additive concentration. This is important as morphologies determine the physical properties of the material. Therefore, this simple solution approach is not only of importance for crystal design of organic functional molecules but also for their materials properties.

We acknowledge financial support by the Max Planck Society. M. Huang thanks the Alexander von Humboldt Foundation for granting a research fellowship, Seed Fund from Ocean University of China, and Fundamental Research Funds for the Central Universities. We thank Julian Jüngling for the reference experiment at pH 10.3.

[1] S. Mann, Angew. Chem., Int. Ed. **39**, 3392 (2000); J. A. A. W. Elemans, A. E. Rowan, and R. J. M. Nolte, J. Am. Chem. Soc. **124**, 1532 (2002).
[2] Y. X. Gao, S. H. Yu, H. Cong, J. Jiang, A. W. Xu, W. F. Dong, and H. Colfen, J. Phys. Chem. B **110**, 6432 (2006); Y. Peng, A. W. Xu, B. Deng, M. Antonietti, and H. Colfen, *ibid.* **110**, 2988 (2006).
[3] Z. Y. Tian, Y. Chen, W. S. Yang, J. N. Yao, L. Y. Zhu, and Z. G. Shuai, Angew. Chem., Int. Ed. **43**, 4060 (2004).
[4] Y. B. Wang, H. B. Fu, A. D. Peng, Y. S. Zhao, J. S. Ma, Y. Ma, and J. N. Yao, Chem. Commun. 1623 (2007).
[5] C. D. Simpson, M. D. Watson, and K. Müllen, J. Mater. Chem. **14**, 494 (2004).
[6] D. Franke, M. Vos, M. Antonietti, N. A. J. M. Sommerdijk, and C. F. J. Faul, Chem. Mater. **18**, 1839 (2006); Y. Zakrevskyy, C. F. J. Faul, Y. Guan, and J. Stumpe, Adv. Funct. Mater. **9**, 835 (2004); Y. Guan, Y. Zakrevskyy, J. Stumpe, M. Antonietti, and C. F. J. Faul, Chem. Commun. 894 (2003).
[7] K. Balakrishnan, A. Datar, R. Oitker, H. Chen, J. Zou, and L. Zang, J. Am. Chem. Soc. **127**, 10496 (2005); Y. Che, A. Datar, K. Balakrishnan, and L. Zang, *ibid.* **129**, 7234 (2007); K. Balakrishnan, A. Datar, W. Zhang, X. Yang, T. Naddo, J. Huang, J. Zuo, M. Yen, J. S. Moore, and L. Zang, *ibid.* **128**, 6576 (2006).
[8] F. C. Meldrum and H. Cölfen, Chem. Rev. **108**, 4332 (2008).

[9] (a) M. Li, H. Schnablegger, and S. Mann, Nature **402**, 393 (1999); (b) C. S. Chan, G. D. Stasio, S. A. Welch, M. Girasole, B. H. Frazer, M. V. Nesterrova, S. Fakra, and J. F. Banfield, Science **303**, 1656 (2004); (c) S. H. Yu, M. Antonietti, H. Cölfen, and J. Hartmann, Nano Lett. **3**, 379 (2003); (d) S. H. Yu, H. Cölfen, and M. Antonietti, J. Phys. Chem. B **107**, 7396 (2003); (e) S. H. Yu, H. Cölfen, and M. Antonietti, Adv. Mater. **15**, 133 (2003); (f) S. H. Yu, H. Cölfen, J. Hartmann, and M. Antonietti, Adv. Funct. Mater. **12**, 541 (2002).
[10] J. H. Adair and E. Suvaci, Curr. Opin. Colloid Interface Sci. **5**, 160 (2000).
[11] D. Gebauer, H. Cölfen, A. Verch, and M. Antonietti, Adv. Mater. **21**, 435 (2009); D. Gebauer, A. Völkel, and H. Cölfen, Science **322**, 1819 (2008); F. C. Meldrum and R. P. Sear, *ibid.* **322**, 1802 (2008); E. M. Pouget, P. H. H. Bomans, J. A. C. M. Goos, P. M. Frederik, G. D. With, and N. A. J. M. Sommerdijk, *ibid.* **323**, 1455 (2009); D. Gebauer, M. Kellermeier, J. D. Gale, L. Bergström, and H. Cölfen, Chem. Soc. Rev. **43**, 2348 (2014).
[12] H. Cölfen, Macromol. Rapid Commun. **22**, 219 (2001).
[13] (a) H. B. Fu, D. B. Xiao, J. N. Yao, and G. Q. Yang, Angew. Chem., Int. Ed. **42**, 2883 (2003); (b) F. Bertorelle, F. Rodrigues, and S. Fery-Forgues, Langmuir **22**, 8523 (2006); (c) T. K. Zhang, J. H. Zhu, H. B. Yao, and S. H. Yu, Cryst. Growth Des. **7**, 2419 (2007); (d) Y. R. Ma, H. G. Börner, J. Hartmann, and H. Cölfen, Chem. - Eur. J. **12**, 7882 (2006); (e) S. Wohlrab, N. Pinna, M. Antonietti, and H. Cölfen, *ibid.* **11**, 2903 (2005).
[14] (a) S. Wohlrab, H. Cölfen, and M. Antonietti, Angew. Chem., Int. Ed. **44**, 4087 (2005); (b) V. Yu, T. Edna Shavit, I. Weissbuch, L. Leiserowitz, and M. Lahav, Cryst. Growth Des. **5**, 2190 (2005); (c) B. D. Hamilton, I. Weissbuch, M. Lahav, M. A. Hillmyer, and M. D. War, J. Am. Chem. Soc. **131**, 2588 (2009); (d) Y. R. Ma, H. Cölfen, and M. Antonietti, J. Phys. Chem. B **110**, 10822 (2006); (e) Y. Jiang, H. F. Gong, D. Volkmer, L. Gower, and H. Cölfen, Adv. Mater. **31**, 3548 (2011); (f) F. Jiang, H. F. Gong, M. Grzywa, D. Volkmer, L. Gower, and H. Cölfen, Adv. Funct. Mater. **23**, 1547 (2013).
[15] Y. R. Ma, G. Mehltretter, C. Plüg, N. Rademacher, M. U. Schmidt, and H. Cölfen, Adv. Funct. Mater. **19**, 2095 (2009); M. Okaniwa, Y. Oaki, and H. Imai, Bull. Chem. Soc. Jpn. **88**, 1459 (2015).
[16] (a) Z. S. Wang, C. H. Huang, F. Y. Li, S. F. Weng, K. Ibrahim, and F. Q. Liu, J. Phys. Chem. B **105**, 4230 (2001); (b) J. Tanaka, Bull. Chem. Soc. Jpn. **36**, 1237–1249 (1963).
[17] H. Langhales, Heteocycles **40**, 477 (1995).
[18] M. Sedlak and H. Cölfen, Macromol. Chem. Phys. **202**, 587 (2001).
[19] M. H. Huang, U. Schilde, M. Kumke, M. Antonietti, and H. Cölfen, J. Am. Chem. Soc. **132**, 3700 (2010).
[20] Y. X. Gao, S. H. Yu, and X. H. Guo, Langmuir **22**, 6125 (2006).
[21] G. Wulff, Z. Kristallogr. - Cryst. Mater. **34**, 449 (1901).
[22] See supplementary material at http://dx.doi.org/10.1063/1.4934704 for SEM image of a cleavage plane for the crystal obtained at pH 9.6 (Figure S1), and also for time-dependent conductivities measurement of PTCAPS crystallization solutions at the different pH values (Figure S2).